

NONNEGATIVE MATRIX FACTORIZATION WITH TRANSFORM LEARNING

Dylan Fagot, Cédric Févotte and Herwig Wendt

CNRS, IRIT, University of Toulouse, France

firstname.lastname@irit.fr

ABSTRACT

Traditional NMF-based signal decomposition relies on the factorization of spectral data which is typically computed by means of the short-time Fourier transform. In this paper we propose to relax the choice of a pre-fixed transform and learn a short-time unitary transform together with the factorization, using a novel block-descent algorithm. This improves the fit between the processed data and its approximation and is in turn shown to induce better separation performance in a speech enhancement experiment.

Index Terms— Nonnegative matrix factorization (NMF), transform learning, single-channel source separation

1. INTRODUCTION

Nonnegative matrix factorization (NMF) has become a privileged approach to spectral decomposition in several fields such as remote sensing and audio signal processing. In the latter field, it has led to state-of-the-art results in source separation [1] or music transcription [2]. The nonnegative data $\mathbf{V} \in \mathbb{R}_+^{M \times N}$ is typically the spectrogram $|\mathbf{X}|$ or $|\mathbf{X}|^{\circ 2}$ of some temporal signal $y \in \mathbb{R}^T$, where $\mathbf{X} \in \mathbb{C}^{M \times N}$ is a short-time Fourier transform (STFT) of y , $|\cdot|$ denotes the entry-wise absolute value and \circ here denotes entry-wise exponentiation. NMF produces the approximate factorization

$$\mathbf{V} \approx \mathbf{W}\mathbf{H}, \quad (1)$$

where $\mathbf{W} \in \mathbb{R}_+^{M \times K}$ is a nonnegative matrix referred to as *dictionary* that contains spectral patterns characteristic of the data while $\mathbf{H} \in \mathbb{R}_+^{K \times N}$ is the nonnegative matrix that contains the *activation coefficients* that approximate the data samples onto the dictionary. The factorization is usually low-rank ($K < \min(M, N)$) but not necessarily so (in which case regularization constraints should apply on \mathbf{W} and/or \mathbf{H}). The decomposition (1) can then be inverted back to the time domain or post-processed in various ways to solve a variety of audio signal processing problems.

In this traditional setting, the STFT (or any regularly-paved time-frequency transform) acts as a pre-processing of the raw temporal data y . This is a potential limitation as any ill-chosen specification of the time-frequency transform may harm the quality of the decomposition. As such, we here propose to learn the transform *together* with the latent factors \mathbf{W} and \mathbf{H} . We propose to address this task by solving an optimization problem of the form

$$\min_{\phi, \mathbf{W}, \mathbf{H}} D(|\phi(y)|^{\circ 2} | \mathbf{W}\mathbf{H}) \quad (2)$$

subject to structure constraints on $\phi : \mathbb{R}^T \rightarrow \mathbb{C}^{M \times N}$ and to non-negativity of \mathbf{W} and \mathbf{H} , and where $D(\cdot | \cdot)$ is a measure of fit.

We present the details of our approach and its connections with the state of the art in Section 2. Section 3 describes an algorithm

that returns stationary points of (2). Section 4 and 5 report results from music decomposition & speech enhancement experiments. In particular, we show that the proposed framework can significantly improve separation accuracy as compared to standard STFT-based NMF.

2. NMF MEETS TRANSFORM LEARNING

2.1. Learning a short-time unitary transform

As a first step, we propose in this paper to gently depart from the traditional STFT setting by restricting the transform $\phi(y)$ to be a short-time unitary transform, likewise the STFT. Let us denote by $\mathbf{Y} \in \mathbb{R}^{M \times N}$ the matrix that contains adjacent & overlapping short-time frames of size M of y and denote by $\Phi_{\text{FT}} \in \mathbb{C}^{M \times M}$ the unitary complex-valued Fourier matrix with coefficients $[\Phi_{\text{FT}}]_{qm} = \exp(j2\pi(q-1)(m-1)/M)$. Under these notations, the power spectrogram of y is simply given by $|\Phi_{\text{FT}}\mathbf{Y}|^{\circ 2}$. As such, traditional NMF may be cast as

$$\min_{\mathbf{W}, \mathbf{H}} D(|\Phi_{\text{FT}}\mathbf{Y}|^{\circ 2} | \mathbf{W}\mathbf{H}) \quad \text{s.t.} \quad \mathbf{W} \geq 0, \mathbf{H} \geq 0, \quad (3)$$

where the notation $\mathbf{A} \geq 0$ expresses the nonnegativity of \mathbf{A} . We propose in this work to relax the pre-fixed transform Φ_{FT} and learn it jointly with \mathbf{W} and \mathbf{H} . This means we consider the following problem

$$\min_{\Phi, \mathbf{W}, \mathbf{H}} D(|\Phi\mathbf{Y}|^{\circ 2} | \mathbf{W}\mathbf{H}) \quad \text{s.t.} \quad \Phi^H \Phi = \mathbf{I}, \mathbf{W} \geq 0, \mathbf{H} \geq 0. \quad (4)$$

We choose at this stage to impose Φ to be unitary likewise the STFT though one could consider relaxing this assumption as well. The unitary constraint implicitly keeps Φ nonsingular and excludes trivial solutions such as $(\Phi, \mathbf{W}, \mathbf{H}) = (\mathbf{0}, \mathbf{0}, \mathbf{0})$ or $(\mathbf{1}_{M \times M}, \mathbf{1}_{M \times 1}, \mathbf{1}_{1 \times M} |\mathbf{Y}|^{\circ 2})$, where $\mathbf{1}_{M \times N}$ denotes the $M \times N$ matrix filled with ones. In this paper, we also choose the measure of fit $D(\cdot | \cdot)$ to be the Itakura-Saito (IS) divergence $D_{\text{IS}}(\mathbf{A} | \mathbf{B}) = \sum_{ij} (a_{ij}/b_{ij} - \log(a_{ij}/b_{ij}) - 1)$. Used with power spectral data, it is known to underly a variance-structured Gaussian composite model that is relevant to the representation of audio signals [3] and has proven an efficient choice for audio source separation, e.g., [4]. However, the proposed framework can accommodate any other measure of fit. We denote by $C(\Phi, \mathbf{W}, \mathbf{H}) = D_{\text{IS}}(|\Phi\mathbf{Y}|^{\circ 2} | \mathbf{W}\mathbf{H})$ the IS-based objective function in problem (4). We refer to the objective described by (4) as TL-NMF, which stands for transform-learning NMF.

2.2. Connection to other works

TL-NMF is inspired by the work of Ravishanker & Bresler [5] on learning sparsifying transforms. Given a collection of data samples \mathbf{Y} (such as images collected in the columns of \mathbf{Y}), their work

Algorithm 1: TL-NMF

Input : \mathbf{Y}, τ
Output: $\Phi, \mathbf{W}, \mathbf{H}$ s.t. $|\Phi \mathbf{Y}|^{\circ 2} \approx \mathbf{W} \mathbf{H}$

Initialize Φ, \mathbf{W} and \mathbf{H}
while $\epsilon > \tau$ **do**
 $\mathbf{W} \leftarrow \mathbf{W} \circ \frac{((\mathbf{W} \mathbf{H})^{\circ -2} \circ |\Phi \mathbf{Y}|^{\circ 2}) \mathbf{H}^T}{(\mathbf{W} \mathbf{H})^{\circ -1} \mathbf{H}^T}$ % MM update [10]
 $\mathbf{H} \leftarrow \mathbf{H} \circ \frac{\mathbf{W}^T ((\mathbf{W} \mathbf{H})^{\circ -2} \circ |\Phi \mathbf{Y}|^{\circ 2})}{\mathbf{W}^T (\mathbf{W} \mathbf{H})^{\circ -1}}$ % MM update [10]
 Normalize \mathbf{W} and \mathbf{H} to remove scale ambiguity
 Compute γ and Ω as in Section 3
 $\Phi \leftarrow \pi(\Phi + \gamma \Omega)$
 Compute stopping criterion ϵ as in Eq. (6)
end

consist in finding an invertible transform Φ such that the output of $\Phi \mathbf{Y}$ is sparse. We are instead looking for a transform Φ such that $|\Phi \mathbf{Y}|^{\circ 2}$ can be well approximated by a NMF. Note that we could more generally consider the problem of finding Φ such that $\Phi \mathbf{Y}$ is low-rank.

TL-NMF can be viewed as finding a one-layer factorizing network, where \mathbf{Y} acts as the raw data, Φ the linear operator, $|\cdot|^{\circ 2}$ the nonlinearity and $\mathbf{W} \mathbf{H}$ the output of the network. As future work, we could imagine fully bridging deep learning and NMF by looking for a cascade of decompositions $f_L(\Phi_L \dots f_1(\Phi_1 \mathbf{Y}))$ such that the output is a NMF. Some recent papers have combined deep learning and NMF but in a different way. For instance, [6] considers a discriminative NMF setting and [7] studies nonnegative auto-encoders.

Finally, note that TL-NMF still operates in a *transformed* domain and is not directly related to synthesis-based NMF models in which the raw data $y(t)$ is modeled as $y(t) = \sum_k c_k(t)$ where the spectrogram of $c_k(t)$ is penalized so as to be closely rank-one [8, 9].

3. ALGORITHM

We describe a block-coordinate descent algorithm that returns stationary points of problem (4). Like the objective function in (3), the objective function $C(\Phi, \mathbf{W}, \mathbf{H})$ is nonconvex and the returned solution depends on initialization. The blocks are the individual variables \mathbf{W} , \mathbf{H} and Φ that are updated in turn until a convergence criterion is met. We use for \mathbf{W} and \mathbf{H} the standard multiplicative IS-NMF updates presented in, e.g., [10], that can be derived from a majorization-minimization procedure. Let us now turn our attention towards the update of Φ . We propose to use a gradient-descent procedure with a line-search step selection followed by a projection onto the unitary constraint, following the approach of [11]. The main benefit of this approach is that it yields an efficient yet simple algorithm for finding a unitary update for Φ .

The gradient of the objective function with respect to (w.r.t.) Φ is given by

$$\nabla \stackrel{\text{def}}{=} \nabla_{\Phi} C(\Phi) = 2(\Delta \circ \mathbf{X}) \mathbf{Y}^T \quad (5)$$

where $\mathbf{X} = \Phi \mathbf{Y}$, $\Delta = \hat{\mathbf{V}}^{\circ -1} - \mathbf{V}^{\circ -1}$, $\mathbf{V} = |\mathbf{X}|^{\circ 2}$, $\hat{\mathbf{V}} = \mathbf{W} \mathbf{H}$. The steepest manifold-dependent descent direction is given by the natural gradient $\Omega = \Phi \nabla^H \Phi - \nabla$. A suitable step-size γ is then chosen according to the Armijo rule so that the projection $\pi(\Phi + \gamma \Omega)$ of the updated transform onto the unitary constraint induces a significant decrease of the objective function [11].

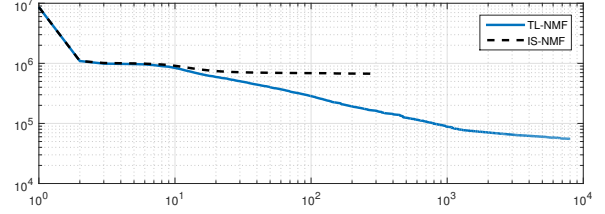


Figure 1: Values of D_{IS} w.r.t. iterations for the experiment reported in Section 4 (log-log scale).

Our block-coordinate descent algorithm is stopped when the relative variation

$$\epsilon^{(i)} = \frac{C(\Phi^{(i)}, \mathbf{W}^{(i)}, \mathbf{H}^{(i)}) - C(\Phi^{(i-1)}, \mathbf{W}^{(i-1)}, \mathbf{H}^{(i-1)})}{C(\Phi^{(i-1)}, \mathbf{W}^{(i-1)}, \mathbf{H}^{(i-1)})} \quad (6)$$

between iteration $i - 1$ and i falls below a given threshold τ . The resulting TL-NMF algorithm is summarized in Algorithm 1. In our experiments, we used nonnegative random values for initializing \mathbf{W} and \mathbf{H} . The transform Φ is initialized with baseline STFT, i.e., $\Phi = \Phi_{\text{FT}}$.

4. MUSIC DECOMPOSITION EXPERIMENT

In this section, we report results obtained with the proposed algorithm for decomposing real audio data $y(t)$ consisting of a 23s excerpt of *Mamavatu* by Susheela Raman that has been downsampled to $f_s = 16\text{kHz}$. \mathbf{Y} is constructed using 40ms-long, 50%-overlapping temporal segments that are windowed with a sine bell. This construction leads to $M = 640$ and $N = 1191$. The behavior of TL-NMF is compared to traditional IS-NMF, which we recall only amounts to TL-NMF with fixed transform Φ_{FT} . The two algorithms are run with the same stopping threshold $\tau = 10^{-5}$ and arbitrary decomposition rank $K = 6$.

Fig. 1 displays the objective function values w.r.t. iterations for the two approaches. They are initialized with the same starting point so that they return the same objective value at iteration $i = 0$. Fig. 1 shows that the proposed algorithm enables to drastically reduce the objective value at convergence as compared to traditional IS-NMF: IS-NMF converges to a divergence of 6.7×10^5 while our variant reaches 5.5×10^4 . This indicates that the proposed algorithm is effective in exploiting the extra flexibility offered by learning the transform Φ jointly with the factorization.

We now examine examples of the atoms returned by TL-NMF (rows ϕ_m of Φ). Fig. 2 displays the real and imaginary parts of the twelve atoms which most contribute to the audio signal, in the sense that they correspond to the twelve largest values of $\|\phi_m \mathbf{Y}\|_2$. It can be observed on the one hand that TL-NMF learns basis elements that do not drastically deviate from the Fourier atoms in that they, e.g., tend to maintain a dominant oscillatory pattern close to the initial Fourier atom. On the other hand, the learnt atoms are also different in that they are neither smooth nor necessarily periodical. They do not necessarily respect phase-quadrature of the real and imaginary part nor respect the Hermitian symmetry that is inherent in Φ_{FT} . Because we are dealing with a nonconvex problem and using a descent algorithm, the estimated transform Φ is inevitably dependent on its Fourier initialization. The effect of this initialization will be more thoroughly studied in future work. However it makes sense in this preliminary work to use Φ_{FT} as the initialization as it corresponds to the traditional NMF setting.

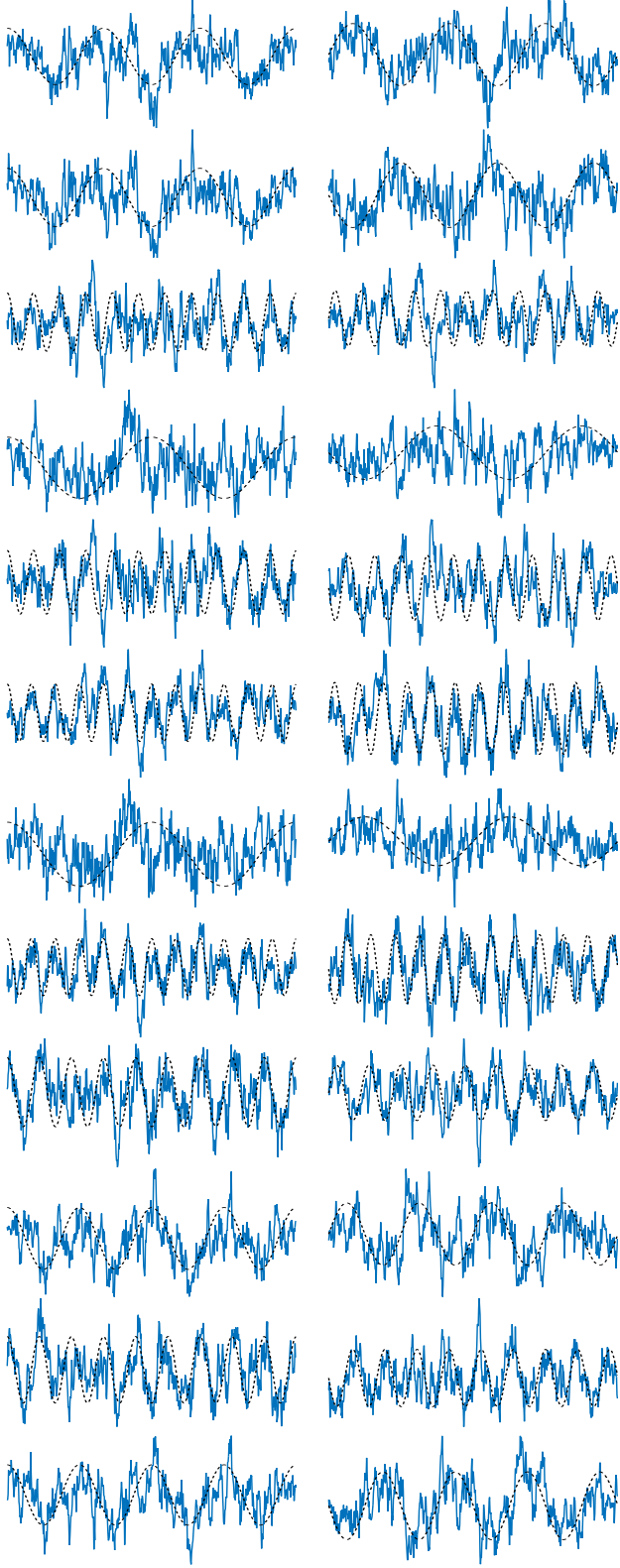


Figure 2: The twelve most significant atoms learnt by TL-NMF (blue solid lines) together with their Fourier initializations (black dashed lines): real (left column) and imaginary parts (right column).

5. SUPERVISED SOURCE SEPARATION

In the previous section, we reported results of exploratory nature that show how TL-NMF is effective in learning a transform. We now examine whether learning an adaptive transform is actually usefully for source separation. To this end, we consider a supervised NMF-based separation setting that follows the approach of [12]. In the following we address the separation of speech from interfering noise, but the method can be applied to any classes of sound.

5.1. Principle

We assume that we are given speech and noise training data $y_s(t)$ and $y_n(t)$ from which we form short-time matrices \mathbf{Y}_s and \mathbf{Y}_n of sizes $M \times N_s$ and $M \times N_n$, as in Section 2.1. Given a noisy speech recording $y(t)$ with short-time matrix \mathbf{Y} , traditional supervised NMF amounts to estimating activation matrices \mathbf{H}_s and \mathbf{H}_n such that

$$\mathbf{V} \approx \mathbf{W}_s \mathbf{H}_s + \mathbf{W}_n \mathbf{H}_n, \quad (7)$$

subject to sparsity of \mathbf{H}_s and \mathbf{H}_n , where $\mathbf{V} = |\Phi_{\text{FT}} \mathbf{Y}|^{\circ 2}$, $\mathbf{W}_s = |\Phi_{\text{FT}} \mathbf{Y}_s|^{\circ 2}$, $\mathbf{W}_n = |\Phi_{\text{FT}} \mathbf{Y}_n|^{\circ 2}$ [12]. Temporal source and noise estimates are then reconstructed in a second step by so-called Wiener filtering [3], based on the spectrogram estimates $\hat{\mathbf{V}}_s = \mathbf{W}_s \mathbf{H}_s$ and $\hat{\mathbf{V}}_n = \mathbf{W}_n \mathbf{H}_n$.

In this section, we generalize this procedure by again learning an optimal transform within the separation procedure. To this end, we propose to build an approximation like Eq. (7) but where the fixed transform $\Phi = \Phi_{\text{FT}}$ is now relaxed and learnt together with \mathbf{H}_s and \mathbf{H}_n . This means we propose to minimize

$$\begin{aligned} C_e(\Phi, \mathbf{H}_s, \mathbf{H}_n) &\stackrel{\text{def}}{=} D_{\text{IS}}(|\Phi \mathbf{Y}|^{\circ 2} \mid |\Phi \mathbf{Y}_s|^{\circ 2} \mathbf{H}_s + |\Phi \mathbf{Y}_n|^{\circ 2} \mathbf{H}_n) \\ &\quad + \lambda_s \|\mathbf{H}_s\|_1 + \lambda_n \|\mathbf{H}_n\|_1 \\ \text{s.t. } &\Phi^H \Phi = \mathbf{I}, \mathbf{H}_s \geq 0, \mathbf{H}_n \geq 0. \end{aligned} \quad (8)$$

The sparsity-inducing ℓ_1 terms on \mathbf{H}_s and \mathbf{H}_n regularize the factorization which becomes potentially overcomplete in the event of large training datasets. Note how Φ now appears in both sides of the data-fitting term $D_{\text{IS}}(\cdot \mid \cdot)$ as the same transform is logically applied to the mixed data \mathbf{Y} and the training data \mathbf{Y}_s and \mathbf{Y}_n . This requires to slightly modify the gradient of C_e w.r.t. Φ as compared to Section 2 and described in next section. After optimization, given $\mathbf{V} = |\Phi \mathbf{Y}|^{\circ 2}$ along with speech and noise spectrogram estimates $\hat{\mathbf{V}}_s = |\Phi \mathbf{Y}_s|^{\circ 2} \mathbf{H}_s$ and $\hat{\mathbf{V}}_n = |\Phi \mathbf{Y}_n|^{\circ 2} \mathbf{H}_n$, temporal estimates may still be produced with Wiener filtering, i.e.,

$$\hat{\mathbf{Y}}_s = \Phi^H \left(\frac{\hat{\mathbf{V}}_s}{\mathbf{V}} \circ (\Phi \mathbf{Y}) \right) \quad (9)$$

followed by standard overlap-adding of the columns of $\hat{\mathbf{Y}}_s$ to return $\hat{y}_s(t)$, and likewise for the noise. This is exactly the same procedure than in traditional NMF-based separation except that the Fourier and inverse-Fourier operations are replaced by Φ and Φ^H .

5.2. Algorithm

Denote $\mathbf{Y}_{\text{train}} = [\mathbf{Y}_s, \mathbf{Y}_n]$, $\mathbf{X}_{\text{train}} = \Phi \mathbf{Y}_{\text{train}}$, $\mathbf{W} = |\mathbf{X}_{\text{train}}|^{\circ 2}$, $\mathbf{H} = [\mathbf{H}_s^T, \mathbf{H}_n^T]^T$ and $\hat{\mathbf{V}} = \mathbf{W} \mathbf{H}$. Given \mathbf{W} , \mathbf{H} can be updated with

Algorithm 2: Supervised TL-NMF

Input : $\mathbf{Y}, \mathbf{Y}_{\text{train}}, \tau$
Output: Φ, \mathbf{H}

Initialize Φ, \mathbf{H}
while $\epsilon > \tau$ **do**

 $\mathbf{V} = |\Phi \mathbf{Y}|^{\circ 2}, \mathbf{W} = |\Phi \mathbf{Y}_{\text{train}}|^{\circ 2}$

 $\mathbf{H} \leftarrow \mathbf{H} \circ \frac{\mathbf{W}^T ((\mathbf{W}\mathbf{H})^{\circ -2} \circ \mathbf{V})}{\mathbf{W}^T (\mathbf{W}\mathbf{H})^{\circ -1} + [\lambda_s \mathbf{1}_{N \times N_s}, \lambda_n \mathbf{1}_{N \times N_n}]^T}$

 Compute γ and Ω as in Section 5.2

 $\Phi \leftarrow \pi(\Phi + \gamma \Omega)$

 Compute stopping criterion ϵ
end

multiplicative rules derived from majorization-minimization as in [10]. We use again a gradient-descent approach for the update of Φ . The gradient of the objective function (8) can be expressed as

$$\nabla_{\Phi} C_e(\Phi, \mathbf{H}) = 2(\Delta \circ \mathbf{X}) \mathbf{Y}^T + 2(\Xi \circ \mathbf{X}_{\text{train}}) \mathbf{Y}_{\text{train}}^T \quad (10)$$

where $\Delta = \hat{\mathbf{V}}^{\circ -1} - \mathbf{V}^{\circ -1}$ and $\Xi = \Delta_e \mathbf{H}^T$ with $\Delta_e = \frac{\hat{\mathbf{V}} - \mathbf{V}}{\mathbf{V}^{\circ 2}}$. Note that the first term of Eq. (10) is the gradient in Eq. (5). The second term is nothing but the gradient of the data-fitting term D_{IS} with its first argument fixed. Based on Eq. (10), we again use a line-search step selection in the steepest natural gradient direction followed by a projection, like in Section 3 and following [11]. The resulting algorithm is summarized in Algorithm 2.

5.3. Speech enhancement experiment

We consider clean speech and noise data from the TIMIT corpus [13] and the CHIME challenge,¹ respectively. For speech training data $y_s(t)$, we use all utterances but the first one in the `train/fcjf0` directory (about 21s in total). For noise training data $y_n(t)$, we use 30s of the file `BGD_150204_010_BUS.CH1.wav`, which contains noise recorded in a bus. A simulated mixed signal $y(t)$ of duration 3s is generated by mixing the remaining speech utterance with another segment of the noise file (as such, the test data is not included in the training data), using a signal-to-noise ratio of -10dB . The audio files sampling frequency is $f_s = 16\text{kHz}$ and short-term matrices \mathbf{Y}, \mathbf{Y}_s and \mathbf{Y}_n are constructed using 40ms-long, 50%-overlapping windowed segments like in Section 4, leading to dimensions $M = 640, N = 149, N_s = 1059$ and $N_n = 1517$. The regularization parameters λ_s and λ_n are arbitrarily set to 10^2 and we again used $\tau = 10^{-5}$.

Our supervised TL-NMF approach is compared to the traditional supervised NMF procedure (with the IS divergence) described in Section 5.1, based on the same training data and using the same regularization parameters (only the transform Φ differs between the two approaches). Source separation performance was assessed using the standard BSS_eval criteria [14]. We also compute the performance criteria obtained by $\hat{y}_s = \hat{y}_n = y/2$ as an indicative baseline. Table 1 reports the comparison results. The results show that the extra adaptability offered by TL-NMF is clearly beneficial as far as source separation capabilities are concerned. Indeed, TL-NMF improves the signal to distortion, interference, and artifact ratios for the speech source by 4.3, 8.0 and 4.1dB, respectively, as compared to traditional IS-NMF. Interestingly, the noise

Method	SDR (dB)		SIR (dB)		SAR (dB)	
	\hat{y}_s	\hat{y}_n	\hat{y}_s	\hat{y}_n	\hat{y}_s	\hat{y}_n
Baseline	-9.50	10.00	-9.50	10.00	∞	∞
IS-NMF	-1.75	-5.41	15.10	12.80	-1.53	-5.12
TL-NMF	2.52	-5.43	23.10	12.60	2.57	-5.13

Table 1: Source separation performance.

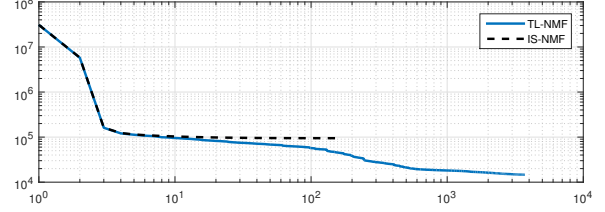


Figure 3: Values of C_e w.r.t. iterations for the experiment reported in Section 5.3 (log-log scale).

separation performance is very similar for TL-NMF and IS-NMF, indicating that the speech source is the one that principally benefits from the adaptive transform. The scores are dependent on the values of λ_s and λ_n but the speech separation performance of TL-NMF was found superior to IS-NMF for all values we tested. This will be reported in a forthcoming long version of this paper.

Fig. 3 displays the values of the objective function C_e returned by supervised TL-NMF and supervised IS-NMF (in which case $\Phi = \Phi_{\text{IT}}$). It clearly indicates that, at convergence, the value of the objective function obtained by the proposed algorithm is nearly one order of magnitude lower than that of IS-NMF: the latter algorithm makes the objective function reach a value of 9.5×10^4 (IS divergence of 6.8×10^4) while our algorithm brings the objective function value down to 1.5×10^4 (IS divergence of 6.0×10^3).

6. CONCLUSION AND FUTURE WORK

We addressed the task of learning the transform underlying NMF-based signal decomposition jointly with the factorization. Specifically, we have proposed a block-coordinate descent algorithm that enables us to find a unitary transform Φ jointly with the dictionary \mathbf{W} and the activation matrix \mathbf{H} . To our knowledge, the proposed algorithm is the first operational procedure for learning a transform in the context of NMF. Our preliminary experiments with real audio data indicate that automatically adapting the transform to the signal pays off when seeking latent factors that accurately represent the data. In particular, the improvement in data fit permits to achieve source separation performance that compares very favorably against the state-of-the-art. Note that although our presentation focused on the processing of audio data, the approach can be adapted to many other settings where NMF is applied to preprocessed data.

Future work will include studying the effect of the initialization of Φ , the influence of the value of K on the learnt transform as well as relaxations of the unitary constraint on Φ , e.g., to nonsingular matrices Φ . Also, the use of alternative optimization strategies that lend themselves well to dealing with nonconvex problems in high dimension, including stochastic gradient descent, will be investigated.

¹http://spandh.dcs.shef.ac.uk/chime_challenge

7. REFERENCES

- [1] P. Smaragdis, C. Févotte, G. Mysore, N. Mohammadiha, and M. Hoffman, “Static and dynamic source separation using nonnegative factorizations: A unified view,” *IEEE Signal Processing Magazine*, vol. 31, no. 3, pp. 66–75, May 2014.
- [2] E. Vincent, N. Bertin, and R. Badeau, “Harmonic and inharmonic nonnegative matrix factorization for polyphonic pitch transcription,” in *Proc. IEEE International Conference on Acoustics, Speech and Signal Processing (ICASSP)*, 2008.
- [3] C. Févotte, N. Bertin, and J.-L. Durrieu, “Nonnegative matrix factorization with the itakura-saito divergence : With application to music analysis,” *Neural Computation*, vol. 21, no. 3, pp. 793–830, 2009.
- [4] B. King, C. Févotte, and P. Smaragdis, “Optimal cost function and magnitude power for NMF-based speech separation and music interpolation,” in *Proc. IEEE International Workshop on Machine Learning for Signal Processing (MLSP)*, 2012.
- [5] S. Ravishankar and Y. Bresler, “Learning sparsifying transforms,” *IEEE Transactions on Signal Processing*, vol. 61, no. 5, pp. 1072–1086, 2013.
- [6] J. L. Roux, J. R. Hershey, and F. Weninger, “Deep NMF for speech separation,” in *Proc. IEEE International Conference on Acoustics, Speech and Signal Processing (ICASSP)*, 2015.
- [7] P. Smaragdis and S. Venkataramani, “A neural network alternative to non-negative audio models,” in *Proc. IEEE International Conference on Acoustics, Speech and Signal Processing (ICASSP)*, 2017.
- [8] C. Févotte and M. Kowalski, “Low-rank time-frequency synthesis,” in *Advances in Neural Information Processing Systems (NIPS)*, 2014.
- [9] H. Kameoka, “Multi-resolution signal decomposition with time-domain spectrogram factorization,” in *Proc. IEEE International Conference on Acoustics, Speech and Signal Processing (ICASSP)*, 2015.
- [10] C. Févotte and J. Idier, “Algorithms for nonnegative matrix factorization with the β -divergence,” *Neural Computation*, vol. 23, no. 9, pp. 2421–2456, 2011.
- [11] J. H. Manton, “Optimization algorithms exploiting unitary constraints,” *IEEE Transactions on Signal Processing*, vol. 50, no. 3, pp. 635–650, 2002.
- [12] P. Smaragdis, B. Raj, and M. V. Shashanka, “Supervised and semi-supervised separation of sounds from single-channel mixtures,” in *Proc. International Conference on Independent Component Analysis and Signal Separation (ICA)*, 2007.
- [13] J. S. Garofolo, L. F. Lamel, W. M. Fisher, J. G. Fiscus, and D. S. Pallett, “Timit acoustic-phonetic continuous speech corpus LDC93S1,” Philadelphia: Linguistic Data Consortium, Tech. Rep., 1993.
- [14] E. Vincent, R. Gribonval, and C. Févotte, “Performance measurement in blind audio source separation,” *IEEE Transactions on Audio, Speech, and Language Processing*, vol. 14, no. 4, pp. 1462–1469, 2006.